



Hybrid Performance of the Pierre Auger Observatory

B.R. DAWSON¹, FOR THE PIERRE AUGER COLLABORATION²

¹*Department of Physics, University of Adelaide, Adelaide 5005, Australia*

²*Observatorio Pierre Auger, Av. San Martín Norte 304, (5613) Malargüe, Mendoza, Argentina*

bruce.dawson@adelaide.edu.au

Abstract: A key feature of the Pierre Auger Observatory is its hybrid design, in which ultra high energy cosmic rays are detected simultaneously by fluorescence telescopes and a ground array. The two techniques see air showers in complementary ways, providing important cross-checks and measurement redundancy. Much of the hybrid capability stems from the accurate geometrical reconstruction it achieves, with accuracy better than either the ground array detectors or a single telescope could achieve independently. We have studied the geometrical and longitudinal profile reconstructions of hybrid events. We present the results for the hybrid performance of the Observatory, including trigger efficiency, energy and angular resolution, and the efficiency of the event selection.

Introduction

The Pierre Auger Observatory is located in the province of Mendoza in western Argentina (35.5°S, 69.3°W). Construction will be complete at the end of 2007, but production data have been collected by the growing observatory since January 2004. At the time of writing, over 1200 of the 1600 water Cherenkov particle detector tanks have been deployed on a 1.5 km triangular grid [1] (Figure 1). Each surface detector (SD) tank contains 12 tonnes of water (10 m² area), and each is equipped with local digitizing electronics (400 MHz sampling rate), solar power, GPS receiver and a radio communication system [2]. The final fluorescence detector (FD) site came into operation in February 2007 on the northern edge of the SD array. Now four sites view the atmosphere above the array, with each site consisting of 6 Schmidt telescopes, a design chosen for improved optical performance. The telescopes each have a field of view of approximately 30° × 30°, mirror area of 12 m², aperture area of 3.8 m² and 440 hexagonal pixels of 1.5° diameter. Pixel signals are digitized with 100 MHz sampling [2].

The unique “hybrid” combination of fluorescence and surface detectors has enormous advantages in all areas of the mission of the Observatory [3]. For example, in our studies of the ultra-high en-

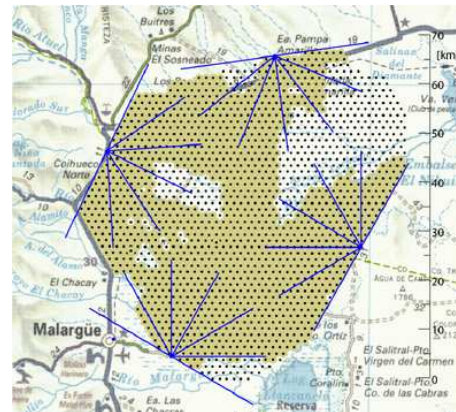


Figure 1: The Observatory in May 2007, showing the positions of the four FD stations and the approximately 1200 deployed SD tanks (shaded region).

ergy cosmic ray (UHECR) energy spectrum [4] the SD provides the energy parameter $S(1000)$, a huge collecting area, 24 hr operation and an easily calculable aperture. The FD provides the conversion between $S(1000)$ and the cosmic ray primary energy, since the FD uses a near-calorimetric technique for determining energy. This avoids calibrating $S(1000)$ via shower simulations, which have uncertainties related to hadronic interaction mod-

els. In anisotropy studies, hybrid data provide high-precision shower arrival directions which are used to cross-check SD-derived directions and to directly measure the SD angular resolution. In mass composition studies, the FD measures the depth of shower maximum X_{\max} , the least indirect of all mass indicators [5]. Meanwhile, hybrid data are being used to calibrate and cross-check several promising mass sensitive parameters measured by the SD alone [6].

The key to the success of hybrid observations is the precise measurements of shower arrival directions. Hybrid data supplements the traditional FD direction fitting method with the arrival time of the shower at the ground measured by a single SD tank. Direction resolution of better than 0.5° not only makes it possible for sensitive anisotropy searches and cross-checks of SD direction assignments, it is also the first step towards high quality measurements of shower longitudinal profiles, and the extraction of X_{\max} and energy [7].

Challenges of a Hybrid Observatory

Some experimental challenges exist in fully realising the promise of the hybrid technique in providing high quality measurements of shower parameters. Most are connected with the FD, since the only data taken from the SD with this technique is the arrival time of the shower at a single tank. The challenges can be divided into three areas - those related to the detector, those related to the atmosphere, and those involved in the reconstruction procedure.

Detector-related challenges include the optical and electronics calibration of the FD system, including its wavelength dependence. We employ an “end-to-end” technique which uses a uniformly illuminated drum positioned at the entrance aperture of a telescope to provide the conversion between a photon flux at the aperture and ADC counts in the electronics [8]. The drum is deployed periodically through the year, and allows measurements at five wavelengths. Nightly relative measurements made with local fixed light sources keep track of any changes between drum calibrations. The current estimate of the systematic uncertainty for shower energy related to the optical calibration is 9.5%. The hybrid method also requires calibration and monitoring of the telescope alignment, and the

synchronization of timing at FD sites and the SD tanks. The former is monitored with star positions and laser shots to a precision of 0.05° ; the latter is monitored and is known at a level of approximately 100 ns.

The atmosphere is our detection medium, and its properties must be carefully monitored. Fluorescence light is produced in proportion to the energy deposited in the atmosphere by shower particles. The efficiency of light production has a dependence on pressure, temperature and humidity. Data from [9] are currently being applied, where the current systematic uncertainty in the absolute fluorescence efficiency is 14%, and an additional uncertainty of 7% is related to pressure, temperature and humidity effects. Improvements in these uncertainties are expected in the near future. The fluorescence light is emitted isotropically from the excited molecules, and is attenuated on its way to the detector by Rayleigh scattering off air molecules and by scattering due to aerosols. Average monthly models of the molecular atmosphere are sufficient to take account of Rayleigh scattering, but treatment of aerosol scattering requires hourly measurements of the characteristics and distribution of aerosols [10]. The Observatory also uses several techniques to detect night-time cloud. The systematic uncertainties in atmospheric attenuation contribute approximately 4% to the systematic uncertainty budget for hybrid estimates of shower energy.

In the algorithm used to reconstruct the longitudinal profile of a shower, one of the important steps is the collection of light in the focal plane of the telescope. Care must be taken to collect the fluorescence light properly (including light from the full lateral width of the shower) without risking the inclusion of night-sky light that dominates away from the image axis. Also, light received at the detector includes direct and scattered Cherenkov light from the atmosphere, which must be accounted for. Systematic uncertainties in these and other parts of the reconstruction method contribute 10% to the total uncertainty in the measured energy. A final correction to the energy takes account of the part of the shower energy that does not contribute proportionally to fluorescence light (e.g. neutrinos, high energy muons). This energy-

Source	Systematic uncertainty
Fluorescence yield	14%
P,T and humidity effects on yield	7%
Calibration	9.5%
Atmosphere	4%
Reconstruction	10%
Invisible energy	4%
TOTAL	22%

Table 1: Systematic uncertainties in determining energy by the hybrid method. Efforts are underway to reduce the main uncertainties in the fluorescence yield, the absolute calibration, and in the reconstruction method.

dependent and mass-dependent “invisible energy” correction has a systematic uncertainty of 4% [11].

Table 1 summarizes the systematic uncertainties in determining energy by the hybrid method.

Trigger Efficiency and Event Selection

Hybrid triggers are formed in near real time, when triggers from fluorescence telescopes are matched with local triggers from individual SD tanks. The local tank trigger, known as a “T2”, is described in [12].

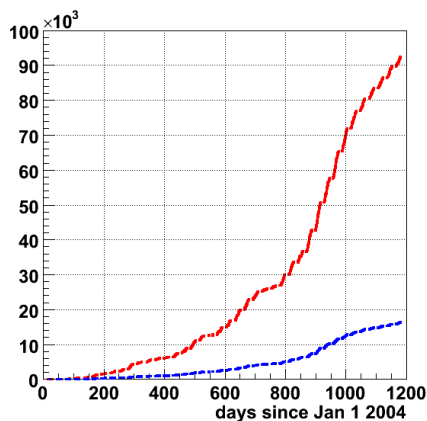


Figure 2: Growth of the hybrid data set. Number of events with angular track length $> 15^\circ$ with geometries successfully reconstructed (top line) (dominated by low energy events); those with well reconstructed longitudinal profiles (quality cuts as in [5]) (bottom).

Simulations of the trigger efficiency have been performed, partly in connection with a hybrid energy spectrum study [13]. The hybrid trigger is fully efficient across the entire SD array above 10^{19} eV, but a significant aperture is available down to energies well below 10^{18} eV. Showers satisfying the triggering criteria can generally be reconstructed to provide good arrival direction information, but not all events provide good estimates of energy or X_{\max} . For example, in the study of the energy dependence of X_{\max} [5], cuts are required on the quality of the observed longitudinal shower profile, as well as cuts to ensure that showers in the sample were not biased in X_{\max} by the limited range of elevations viewed by the FD telescopes. The same “quality cuts” were applied to showers used in the hybrid calibration of the SD energy parameter $S(1000)$ [4].

Figure 2 shows the growth of the hybrid data set since January 2004, including events successfully passing the geometry reconstruction stage, and the number with well-reconstructed longitudinal profiles.

Geometry and Profile Resolution

The line of triggered pixels in an FD camera defines a plane in space containing the shower axis and a point representing the FD, known as the shower-detector plane (SDP). The orientation of the shower axis within the SDP is determined using timing information. With an FD alone, the reconstruction of the axis within the SDP can sometimes suffer from degeneracy related to the inability to detect changes in the angular speed of the shower image across the FD camera. The hybrid technique breaks this degeneracy by including the arrival time of the shower at ground level, data provided by a single SD tank near the shower axis [7].

Simulations have been performed to estimate the geometry and shower profile resolution. A sample of showers with energies in the range $10^{18} - 10^{19}$ eV have been simulated with a E^{-2} differential energy spectrum, thus including a rough allowance for the growing FD aperture with energy. With minimum cuts (angular track length $> 15^\circ$, reconstructed tank-core distance < 2 km) the median and 90% core location errors are 35 m and 150 m respectively, and the median and 90% arrival direction errors are 0.35° and 0.95° . The pro-

file resolution results are shown in Figure 3. Quality cuts described in [5] have been applied for these plots.

At the higher energies the observatory has measured a number of showers observed by two (or more) FD sites. This offers an opportunity to cross-check these simulation results, though two caveats apply. First, the event statistics are low, especially after standard quality cuts are applied to each of the views of a shower. Secondly, the steeply falling energy spectrum means that many of these “stereo” events have a lower than average quality image in at least one of the two FD eyes. In any case, the single-eye energy and X_{\max} resolution figures derived from stereo events (11% and 18 g cm^{-2} respectively) are entirely consistent with simulation results.

References

- [1] T. Suomijarvi [Pierre Auger Collaboration], these proceedings (#299).
- [2] J. Abraham et al. [Pierre Auger Collaboration] Nucl. Inst. Meth. A. **523**, 50 (2004)
- [3] P. Sommers, Astropart. Phys. **3**, 349 (1995)
- [4] M. Roth [Pierre Auger Collaboration], these proceedings (#313).
- [5] M. Unger [Pierre Auger Collaboration], these proceedings (#594).
- [6] M. Healy [Pierre Auger Collaboration], these proceedings (#596).
- [7] B.R. Dawson, H.Y. Dai, P. Sommers and S. Yoshida, Astropart. Phys. **5**, 239 (1996)
- [8] R. Knapik [Pierre Auger Collaboration], these proceedings (#393).
- [9] M. Nagano *et al.*, Astropart. Phys. **22**, 235 (2004).
- [10] S. Ben-Zvi [Pierre Auger Collaboration], these proceedings (#399).
- [11] T. Pierog, R. Engel and D. Heck, Czech. J. Phys. **56**, A161-A172 astro-ph/060219 (2006).
- [12] D. Allard [Pierre Auger Collaboration], Proc. 29th ICRC (Pune) **7**, 287 (2005).
- [13] L. Perrone [Pierre Auger Collaboration], these proceedings (#316).

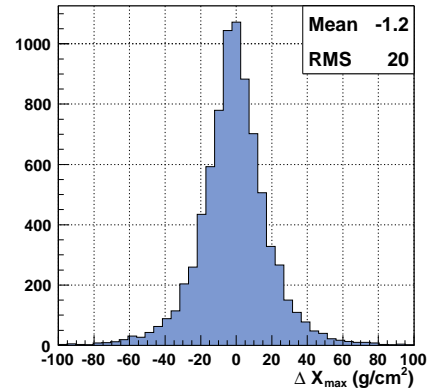
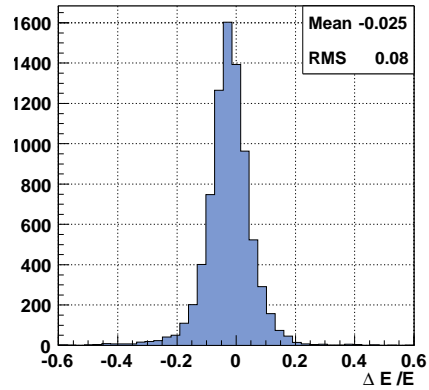


Figure 3: Resolution results for $10^{18} - 10^{19} \text{ eV}$ (E^{-2} differential spectrum). Applying cuts from [5], statistical resolution of 8% in energy and 20 g cm^{-2} in X_{\max} is achieved.